*Axion cold dark matter

기초과학연구원
Institute for Basic Science

*Magnetosphere

conversion

*Resonant

region

10 km

Axion → Photon

I become massive

a

γ

Radio

Probing dark matter and baryon asymmetry of the universe by SKA-like and LISA-like experiments

Fa Peng Huang

IBS-CTPU

(move to Washington University in St. Louis from this Aug.)

SUSY 2019 @Texas A&M University in Corpus Christi, USA

23th May, 2019

SKA

$m_a \sim m_\gamma$

Motivation

Long-lasting problems in our understanding of particle cosmology (such as the dark matter and the baryon asymmetry of the universe), and no evidence of new physics at LHC and dark matter direct search may just point us towards new approaches, especially the Radio telescope experiments (SKA, FAST, GBT…) and the Laser Interferometer experiments (LISA, Tianqin/Taiji…)

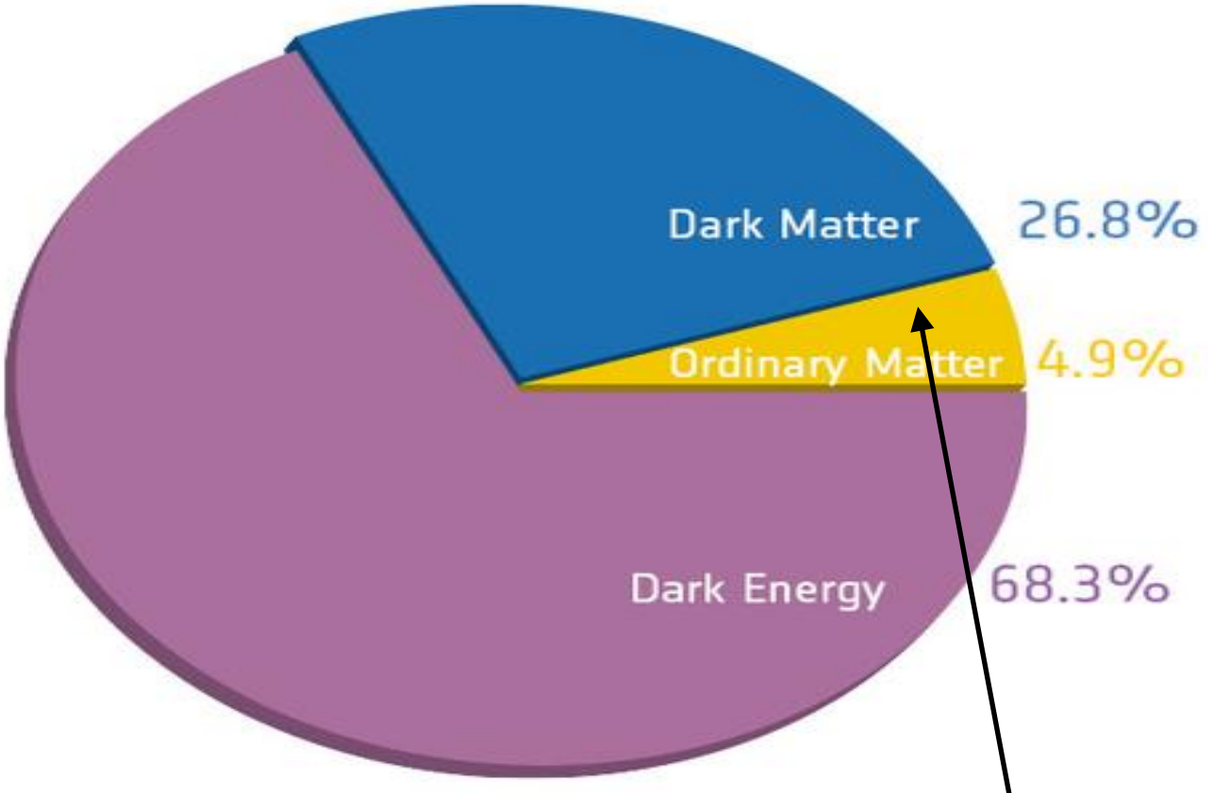

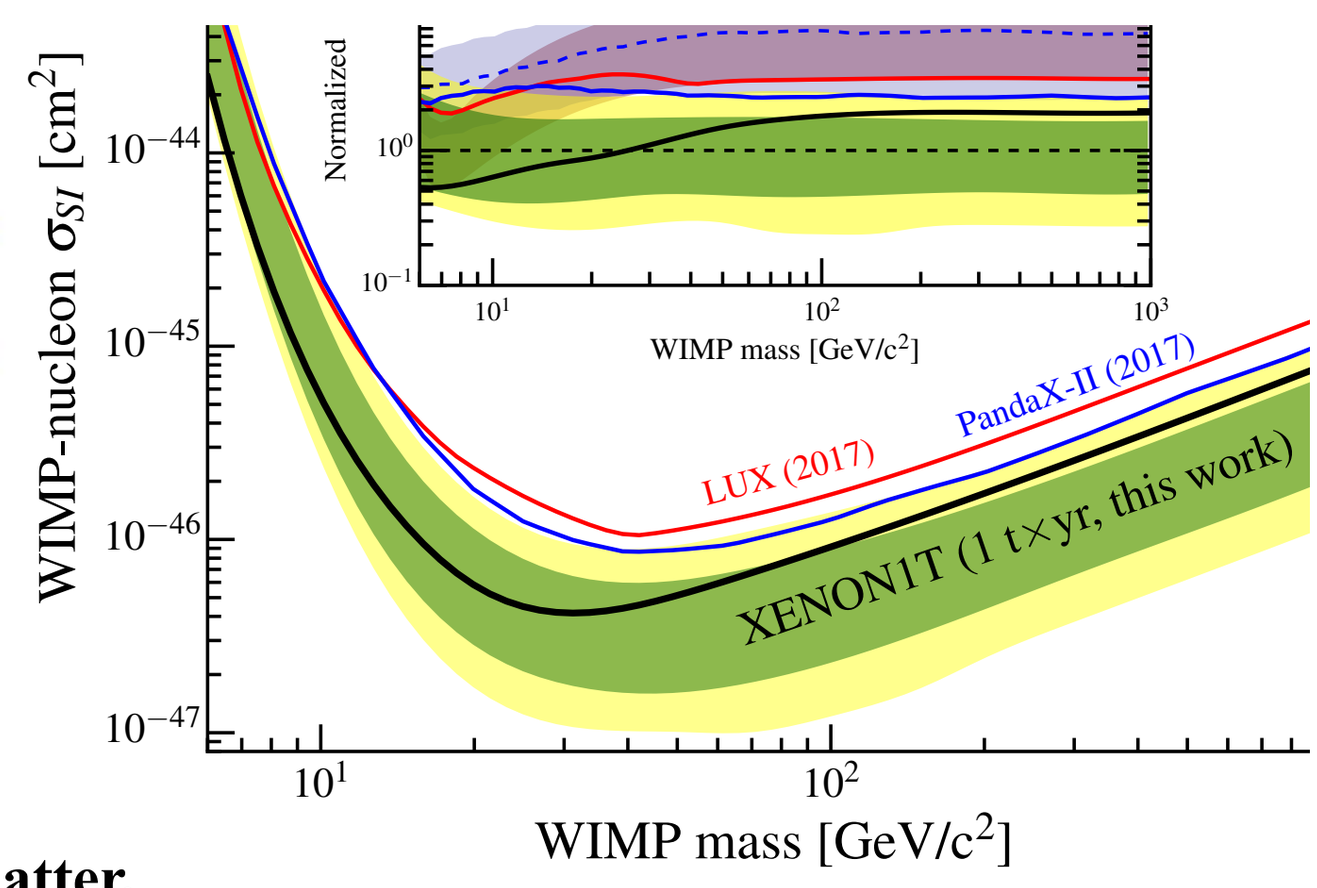

Why negligible antimatter, (baryon asymmetry of the universe)?

Phys.Rev.Lett. 121 (2018) no.11, 111302

Motivation

EW phase transition and baryogenesis: LISA, Tianqin/Taiji

QCD phase transition and axion cold dark matter: SKA, FAST, GBT(radio telescope)

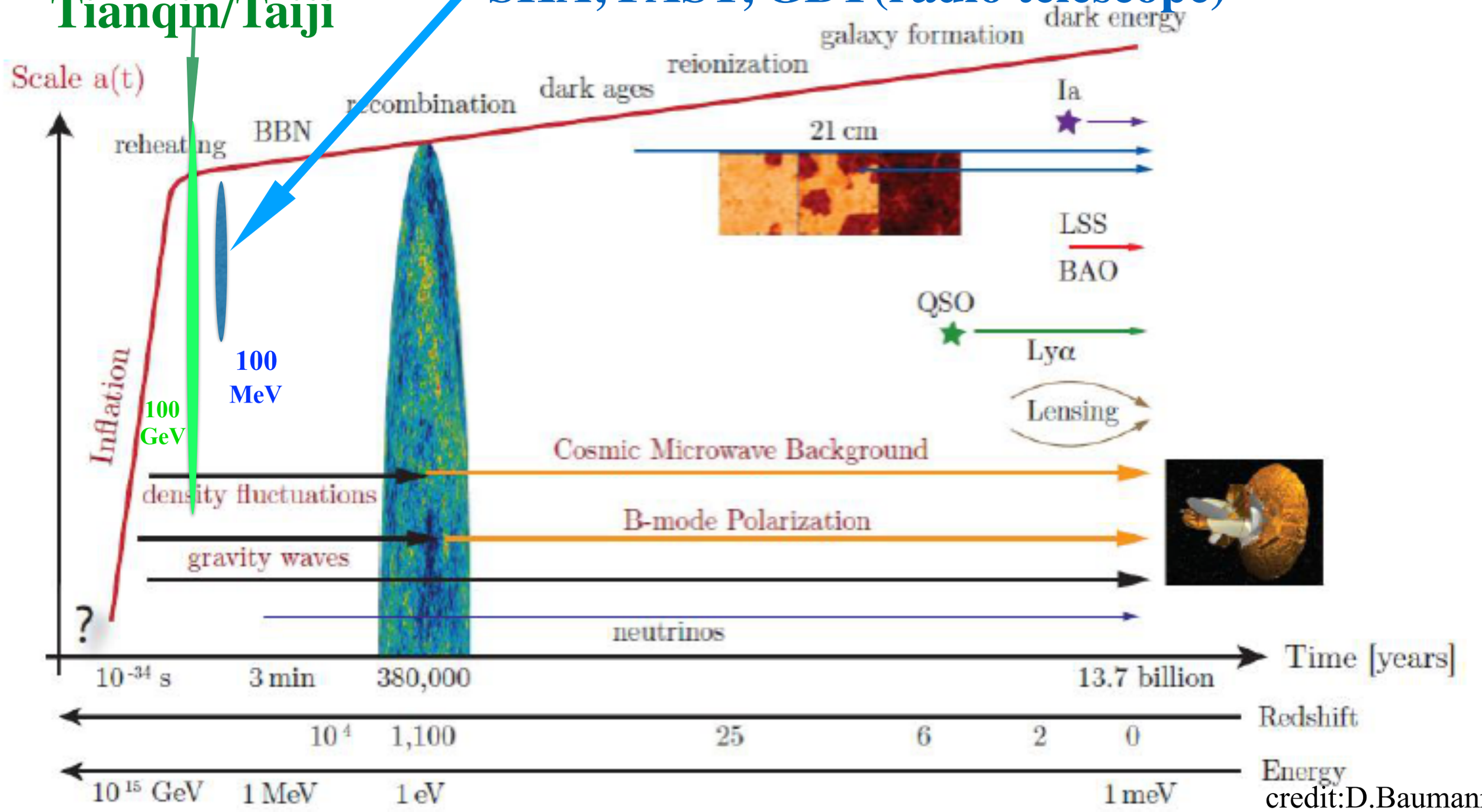

credit:D.Baumann

The Square Kilometer Array (SKA)

Early science observations are expected to start in 2020 with a partial array.

credit: SKA website

The Five-hundred-meter Aperture Spherical radio Telescope (FAST)

969 days in operation since 25 Sep. 2016

Credit:FAST website

The Green Bank Telescope (GBT)

GBT is running observations roughly 6,500 hours each year

credit:GBT website

Laser Interferometer Space Antenna (LISA)

Launch in 2034

credit:LISA website

Explore the axion cold dark matter

Axion or axion-like dark matter motivated from strong-CP problem or string-theory is still one of the most attractive and promising dark matter candidate.

See Peter Graham's talk for axion cold dark matter

We firstly study using the SKA-like experiments to explore the resonant conversion of axion cold dark matter to radio signal from magnetized astrophysical sources, such as neutron star, magnetar and pulsar.

FPH, K. Kadota, T. Sekiguchi, H. Tashiro, Phys.Rev. D97 (2018) no.12, 123001, arXiv:1803.08230

*Axion cold dark matter

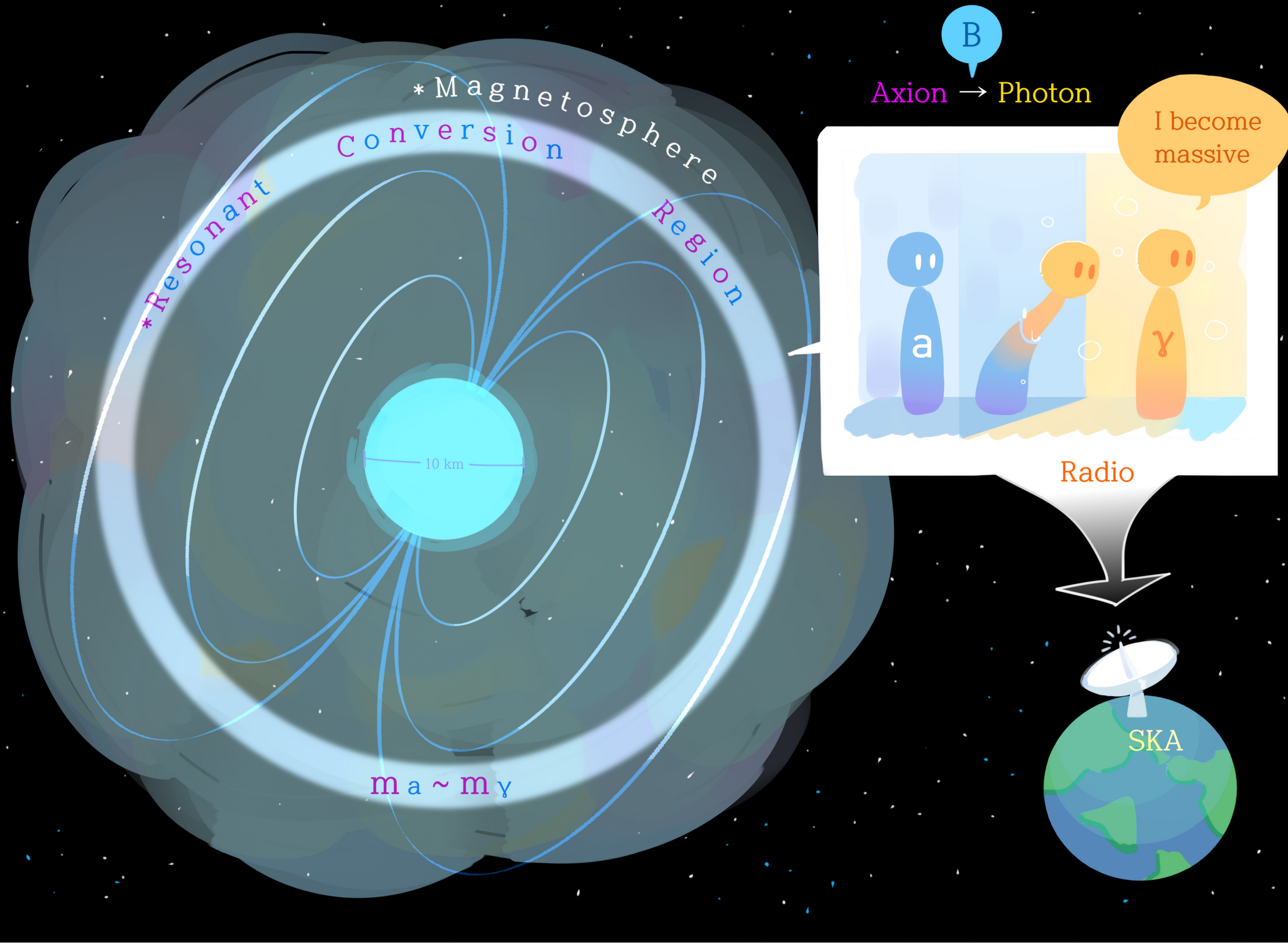

FPH, **K. Kadota, T. Sekiguchi, H. Tashiro, Phys.Rev. D97 (2018) no.12, 123001**

Radio telescope search for the resonant conversion of cold dark matter axions from the magnetized astrophysical sources

Three key points:

- **Cold DM is composed of non-relativistic axion or axion-like particles, and can be accreted around the neutron star**
- **Neutron star (or pulsar and magnetar) has the strongest position-dependent magnetic field in the universe**
- **Neutron star is covered by magnetosphere and photon becomes massive in the magnetosphere**

Quick sketch of the neutron star size

Upcoming Half Marathons in Corpus Christi, TX - Running in the USA

https://runningintheusa.com/classic/list/corpus%20christi-tx/upcoming/half-marathon

1. Surf-N-Turf Race. Jan 25, 2020. Saturday. 13.1M, 10K, 5K run. Race Link. **Corpus Christi**, **TX**. City Location. Nueces County, **TX**. details update save claim.

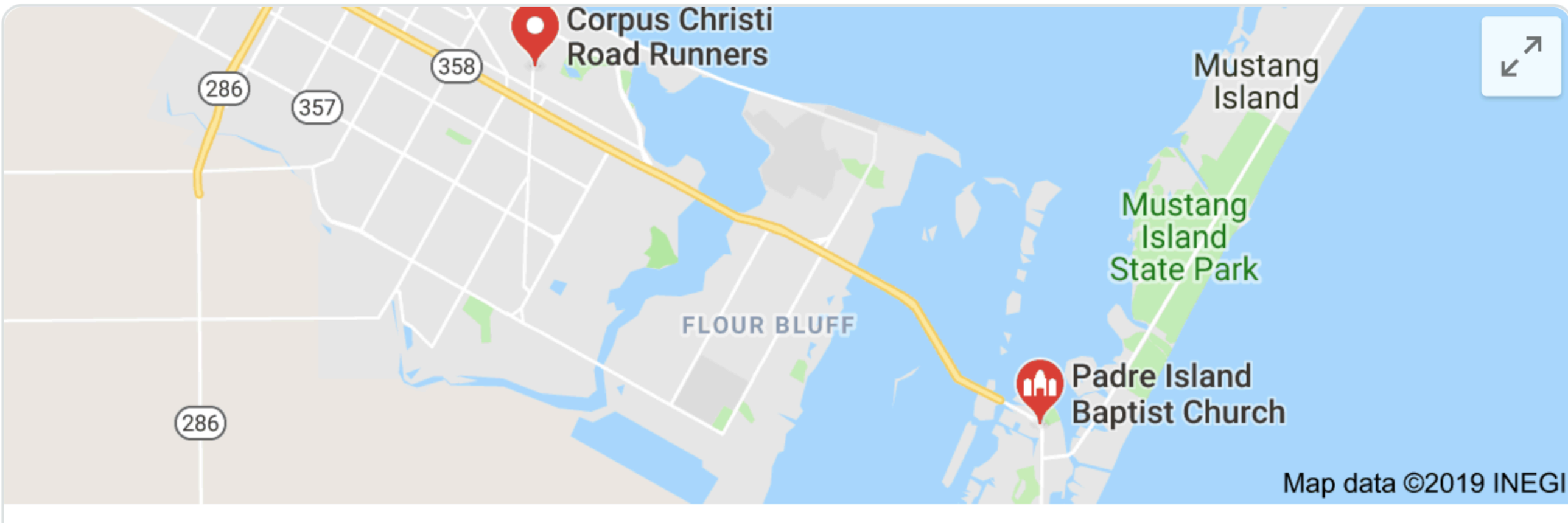

Strong magnetic field in the magnetosphere of Neutron star, Pulsar, Magnetar: the strongest magnetic field in the universe

1. **Mass:from 1 to 2 solar mass**

2. **Radius:** $r_0 \sim 10 - 20\mathrm{km}$

   The typical diameter of neutron star is just half Marathon.

3. **Strongest magnetic field at the suface of the neutron star**

$$B_0 \approx 10^{12} - 10^{15}\mathrm{G}$$

$$B_0 \sim 3.3 \times 10^{19}\sqrt{P\dot{P}} \quad \mathrm{G}$$

P is the period of neutron star

4. **Neutron star is surrounded by large region of magnetosphere, where photon becomes massive.**

$$r \sim 100 r_0$$

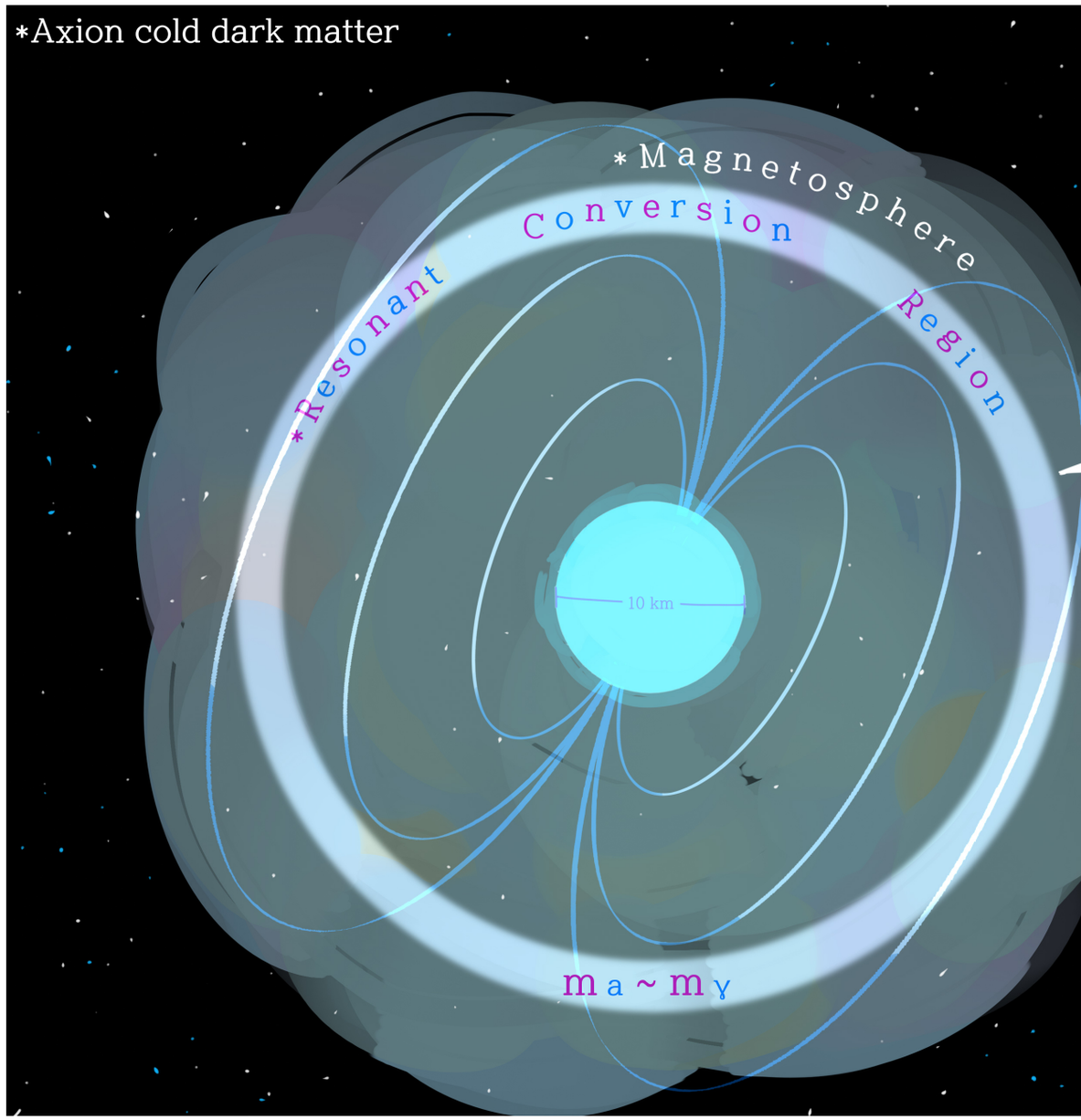

Axion-photon conversion in magnetosphere

The Lagrangian for axion-photon conversion the magnetosphere

$$L = -\frac{1}{4}F_{\mu\nu}F^{\mu\nu} + \frac{1}{2}(\partial_\mu a \partial^\mu a - m_a^2 a^2) + L_{\rm int} + L_{\rm QED}$$

$$L_{\rm QED} = \frac{\alpha^2}{90m_e^4}\frac{7}{4}(F_{\mu\nu}\tilde{F}^{\mu\nu})^2$$

Massive Photon: In the magnetosphere of the neutron star, photon obtains the effective mass in the magnetized plasma.

$$m_\gamma^2 = Q_{\rm pl} - Q_{\rm QED}$$

$$Q_{\rm QED} = \frac{7\alpha}{45\pi}\omega^2\frac{B^2}{B_{\rm crit}^2}$$

$$Q_{\rm plasma} = \omega_{\rm plasma}^2 = 4\pi\alpha\frac{n_e}{m_e}$$

$$\frac{Q_{\rm pl}}{Q_{\rm QED}} \sim 5\times 10^8\left(\frac{\mu{\rm eV}}{\omega}\right)^2\frac{10^{12}\ {\rm G}}{B}\frac{1\ \ {\rm sec}}{P}$$

$$L_{\rm int} = \frac{1}{4}g\tilde{F}^{\mu\nu}F_{\mu\nu}a = -g\mathbf{E}\cdot\mathbf{B}a,$$

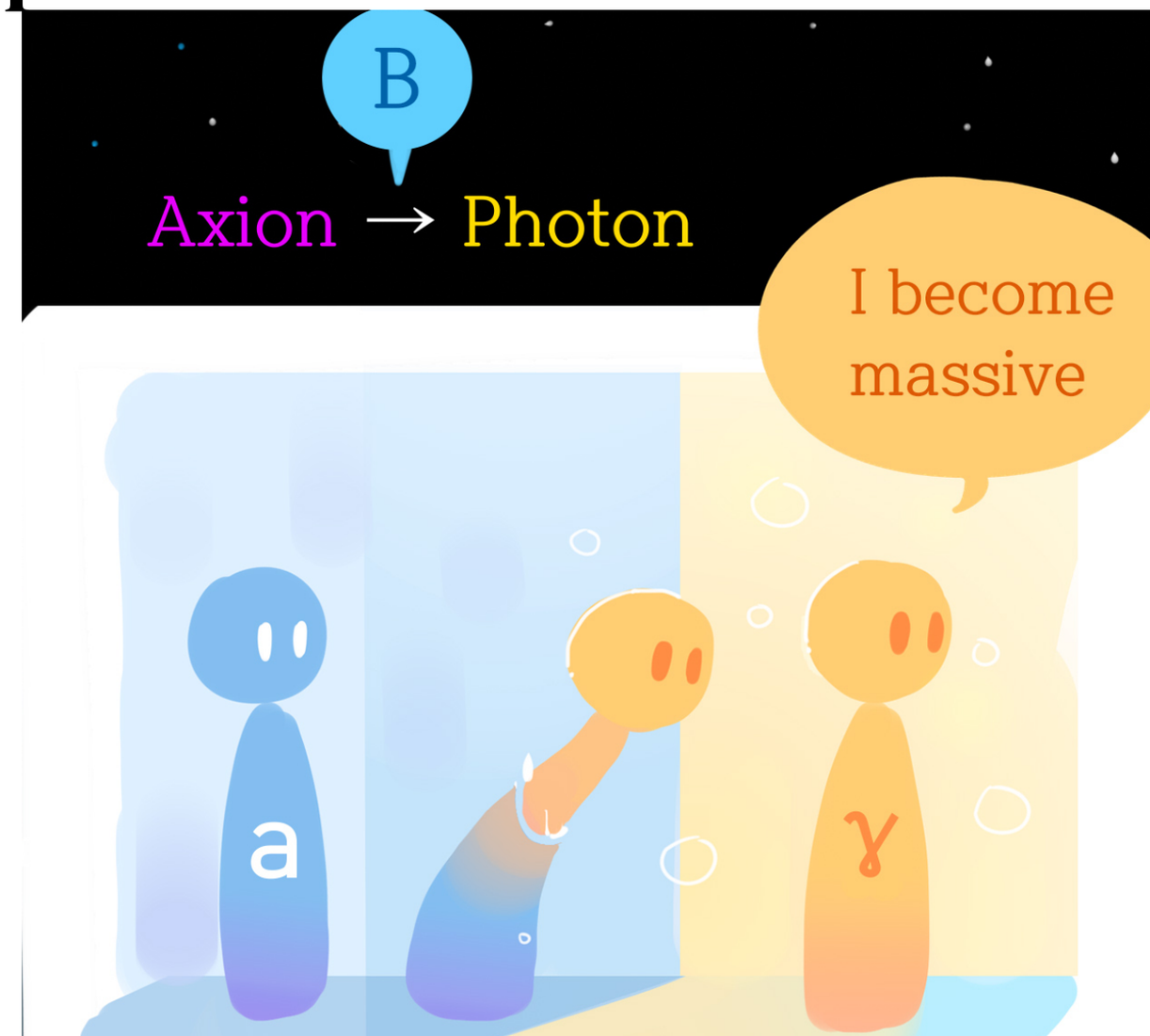

Axion-photon conversion in magnetosphere

The axion-photon conversion probability

$$p_{a\to\gamma} = \sin^2 2\tilde{\theta}(z)\,\sin^2[z(k_1-k_2)/2]$$

$$\sin 2\tilde{\theta} = \frac{2gB\omega}{\sqrt{4g^2B^2\omega^2 + (m_\gamma^2 - m_a^2)^2}}$$

$$m_\gamma^2(r) = 4\pi\alpha\frac{n_e(r)}{m_e}$$

Here, for non-relativistic axion cold dark matter, the QED mass is negligible compared to plasma mass.

$$B(r) = B_0\left(\frac{r}{r_0}\right)^{-3}$$

$$n_e(r) = n_e^{\mathrm{GJ}}(r) = 7\times10^{-2}\,\frac{1s}{P}\,\frac{B(r)}{1\ \mathrm{G}}\,\frac{1}{\mathrm{cm}^3}$$

Here, we choose the simplest magnetic field configuration and electron density distribution to clearly see the underlying physics.

Thus, the photon mass is position r dependent, and within some region the photon mass is close to the axion DM mass.

The Adiabatic Resonant Conversion

The resonance radius is defined at the level crossing point

$$m_\gamma^2(r_{\rm res}) = m_a^2$$

At the resonance, $|m_\gamma^2 - m_a^2| \ll gB\omega$ and $m_{1,2}^2 \approx m_a^2 \pm gB\omega$.

Within the resonance region, the axion-photon conversion rate is greatly enhanced due to large mixing angle.

$$\sin 2\tilde{\theta} = \frac{(2gB\omega/m_\gamma^2)}{\sqrt{(4g^2B^2\omega^2/m_\gamma^4) + (1-(m_a/m_\gamma)^2)^2}} \equiv \frac{c_1}{\sqrt{c_1^2 + (1-f(r))^2}},$$

N.B. Only for the non-relativistic axion, the resonant conversion can be achieved. For relativistic axion, QED effects make it impossible.

The adiabatic resonant conversion requires the resonance region is approximately valid inside the resonance width. Coherent condition is also needed.

$$\delta r > l_{\rm osc} = \frac{2\pi}{|k_1 - k_2|_{\rm res}}$$

$$|d\tilde{\theta}/dr|_{\rm res} < l_{\rm osc}^{-1}$$

$$|d\ln f/dr|_{\rm res}^{-1} > 650[m]\left(\frac{m_a}{\mu{\rm eV}}\right)^3\left(\frac{v_{\rm res}}{10^{-1}}\right)\left(\frac{1/10^{10}\ {\rm GeV}}{g}\right)^2 \times \left(\frac{10^{12}\ {\rm G}}{B(r_{\rm res})}\right)^2\left(\frac{\mu{\rm eV}}{\omega}\right)^2$$

Adiabatic resonant conversion is essential to observe the radio signal.

Radio Signal

Line-like radio signal for non-relativistic axion conversion:

$$\nu_{\rm peak} \approx \frac{m_a}{2\pi} \approx 240 \frac{m_a}{\mu eV} {\rm MHz}$$ **1 GHz ~ 4 μeV**

The FAST covers 70 MHz–3 GHz, the SKA covers 50 MHz–14 GHz, and the GBT covers 0.3–100 GHz, so that the radio telescopes can probe axion mass range of 0.2–400 μeV

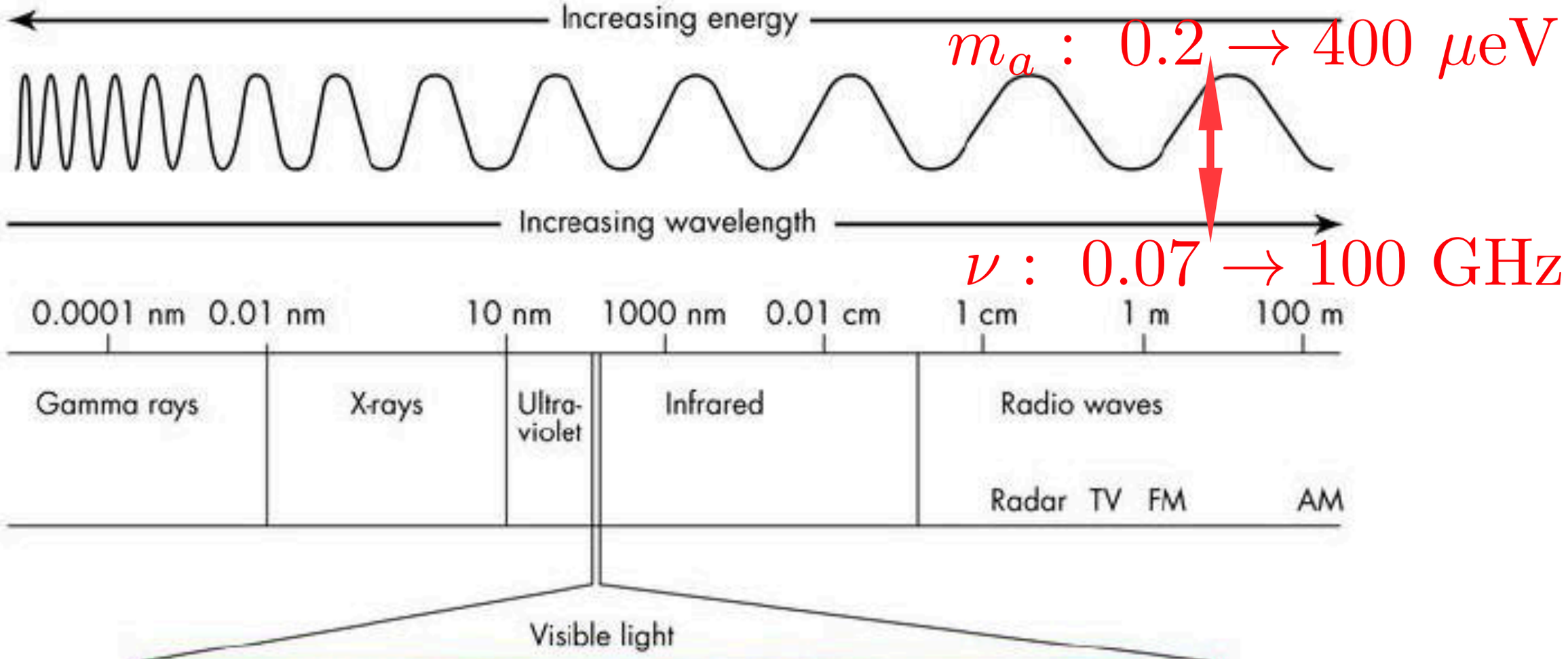

Radio Signal

Signal: For adiabatic resonant conversion, and the photon flux density can be estimated to be of order

$$S_\gamma = \frac{dE/dt}{4\pi d^2 \Delta\nu} \sim 4.2\mu Jy \frac{\left(\frac{r_{\rm res}}{100\ {\rm km}}\right)\left(\frac{M}{M_{\rm sun}}\right)\left(\frac{\rho_a}{0.3\ {\rm GeV/cm^3}}\right)\left(\frac{10^{-3}}{v_0}\right)\left(\frac{g}{1/10^{10}\ {\rm GeV}}\right)\left(\frac{B(r_{\rm res})}{10^{12}\ {\rm G}}\right)\left(\frac{\omega}{\mu{\rm eV}}\right)\left(\frac{\mu{\rm eV}}{m_a}\right)^2}{\left(\frac{d}{1\ {\rm kpc}}\right)^2\left(\frac{m_a/2\pi}{\mu{\rm eV}/2\pi}\right)\left(\frac{v_{\rm dis}}{10^{-3}}\right)},$$

where d represents the distance from the neutron star to us. The photon flux peaks around the frequency $\nu_{\rm peak} \sim m_a/2\pi$, and $\Delta\nu \sim \nu_{\rm peak} v_{\rm dis}$ represents the spectral line broadening around this peak frequency due to the DM velocity dispersion $v_{\rm dis}$.

Sensitivity: The smallest detectable flux density of the radio telescope (SKA, FAST, GBT) is of order

$$S_{\rm min} \approx 0.29\mu Jy \left(\frac{1\ {\rm GHz}}{\Delta B}\right)^{1/2} \left(\frac{24\ {\rm hrs}}{t_{\rm obs}}\right)^{1/2} \left(\frac{10^3\ {\rm m^2/K}}{A_{\rm eff}/T_{\rm sys}}\right)$$

Radio Signal

Signal: For a trial parameter set, $B_0 = 10^{15}$ G, $m_a = 50\ \mu$eV

$P = 10$ s, $g = 5 \times 10^{-11}$ GeV^{-1}, $r_0 = 10$ km, $M = 1.5 M_{\rm sun}$, $d = 1$kpc

satisfies the conditions for the adiabatic resonance conditions and the existed axion search constraints with signal $S_\gamma \sim 0.51$ μJy**.**

Sensitivity: $S_{\rm min} \sim 0.48 \mu Jy$ for the SKA1

$S_{\rm min} \sim 0.016 Jy$ for the SKA2 with 100 hour observation

SKA-like experiment can probe the axion dark matter and the axion mass which corresponds to peak frequency.

More detailed study taking into account astrophysical uncertainties and more quantitatively numerical analysis for our adiabatic resonance conversion scenario is still working in progress.

*Axion cold dark matter

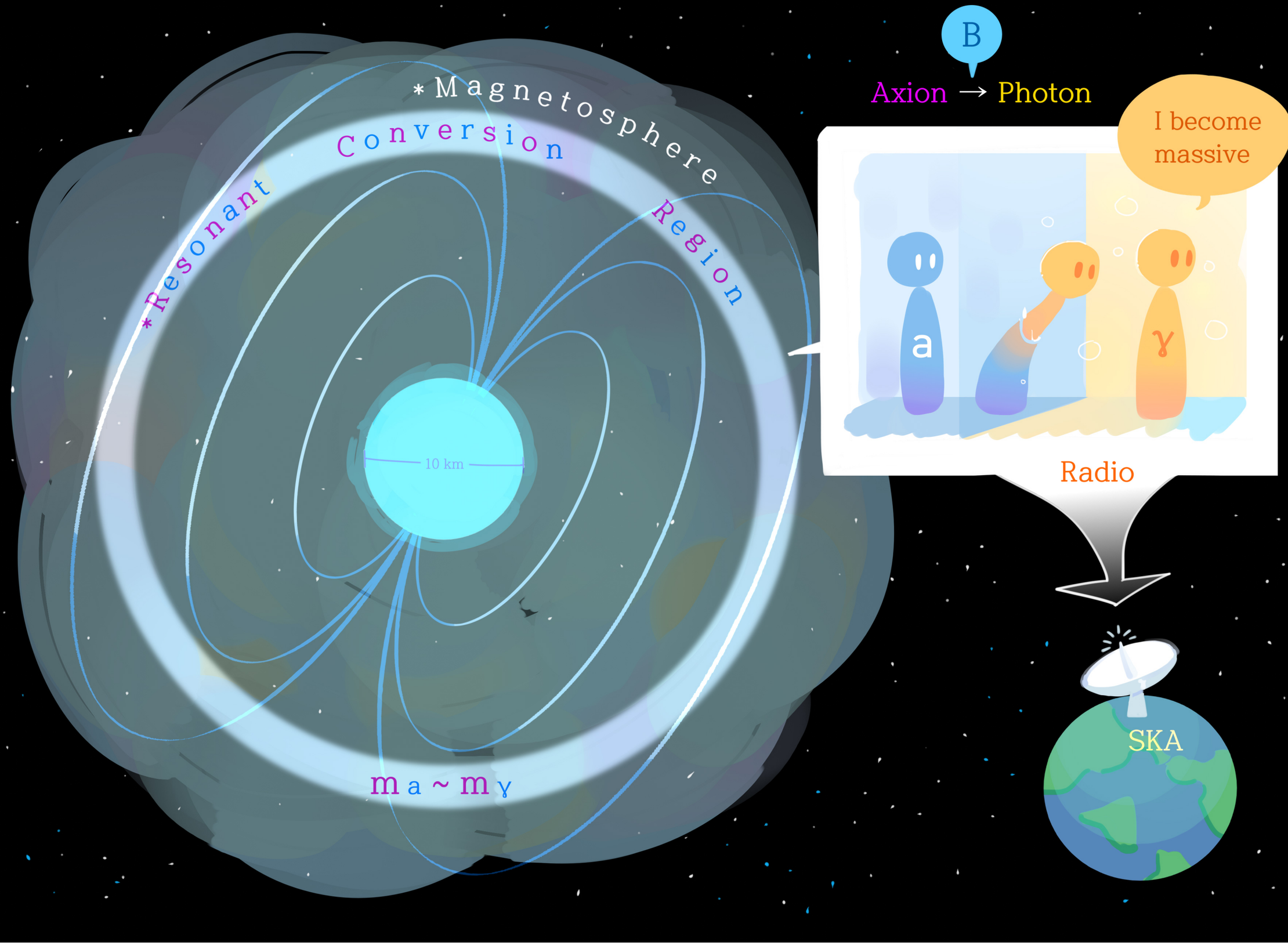

FPH, **K. Kadota, T. Sekiguchi, H. Tashiro, Phys.Rev. D97 (2018) no.12, 123001**

Comments on the radio probe of axion dark matter

1. Astrophysical uncertainties:the magnetic profile of the neutron star, the dark matter density around the neutron star, the location of the neutron star, the velocity dispersion, the plasma mass, background including the optimized bandwidth…

2. There are more and more detailed studies after our first estimation on the radio signal:

arXiv:1804.03145 by Anson Hook, Yonatan Kahn, Benjamin R. Safdi, Zhiquan Sun where they consider more details and extremely high dark matter density around the neutron star, thus the signal is more stronger.

arXiv:1811.01020 by Benjamin R. Safdi, Zhiquan Sun, Alexander Y. Chen

arXiv:1905.04686,Thomas, D.P.Edwards,Marco Chianese, Bradley J. Kavanagh, Samaya M. Nissanke, Christoph Weniger, where they consider multi-messenger of axion dark matter detection. Namely, using LISA to detect the dark matter density around the neutron star, which can determine the radio strength detected by SKA

Powerful LISA experiments

- **The true shape of Higgs potential (Exp: complementary check with CEPC)**
- **Baryon asymmetry of the universe (baryogenesis)**
- **Gravitational wave (Exp:LISA 2034)**
- **Dark Matter blind spots** **Phys.Rev. D98 (2018) no.9, 095022,**
  FPH,Jianghao Yu
- **Asymmetry dark matter**

(The cosmic phase transition with Q-balls production mechanism can explain the baryogenesis and DM simultaneously, where constraints on DM masses and reverse dilution are significantly relaxed.
FPH, Chong Sheng Li, Phys.Rev. D96 (2017) no.9, 095028)

LISA in synergy with CEPC helps to explore the evolution history of the universe at several hundred GeV temperature, dark matter and baryogenesis.

Current particle collider has no ability to unravel the true potential of the Higgs boson, we need new experiments.

Particle approach

we can build more powerful colliders, such as planned CEPC/SppC, FCC etc.

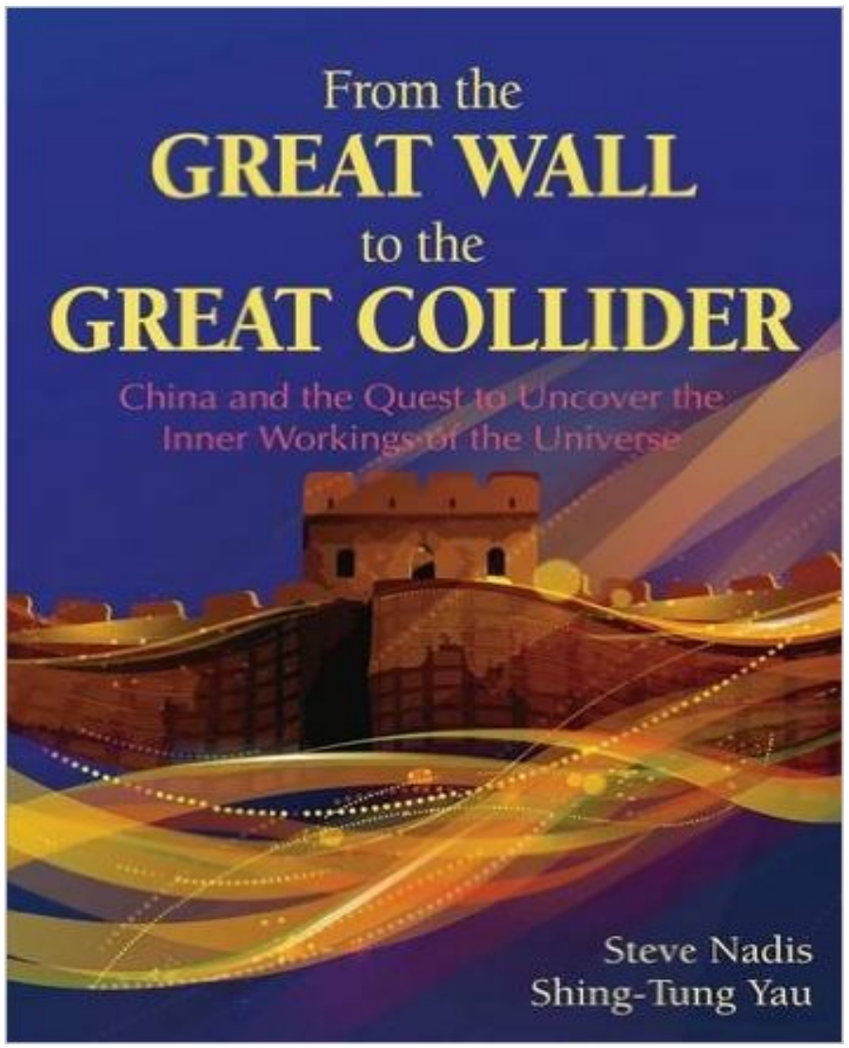

Relate by EW phase transition/ baryogenesis

Double test on the Higgs potential and baryogenesis

Wave approach

GW detectors can test Higgs potential as complementary approach. (LISA launch 2034)

EW baryogenesis in a nutshell

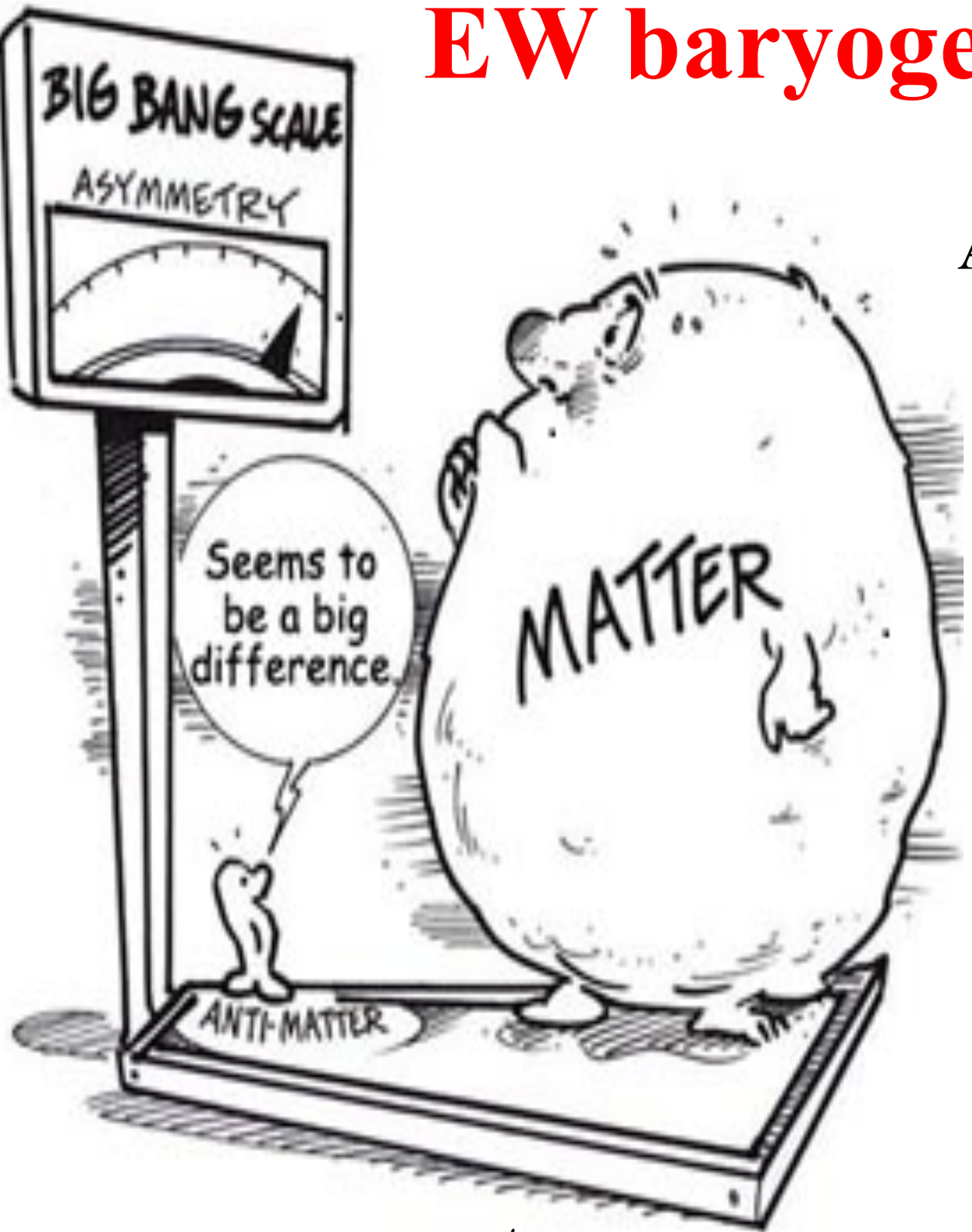

A long standing problem in particle cosmology is the origin of baryon asymmetry of the universe (BAU).

After the discovery of the Higgs boson by LHC and gravitational waves (GW) by aLIGO, EW baryogenesis becomes a timely and testable scenario for explaining the BAU.

$$\eta_B = n_B/n_\gamma = 5.8 - 6.6 \times 10^{-10} \quad \text{(CMB, BBN)}$$

EW baryogenesis:

SM technically has all the three elements for baryogenesis , (Baryon violation, C and CP violation, Departure from thermal equilibrium or CPT violation) but not enough.

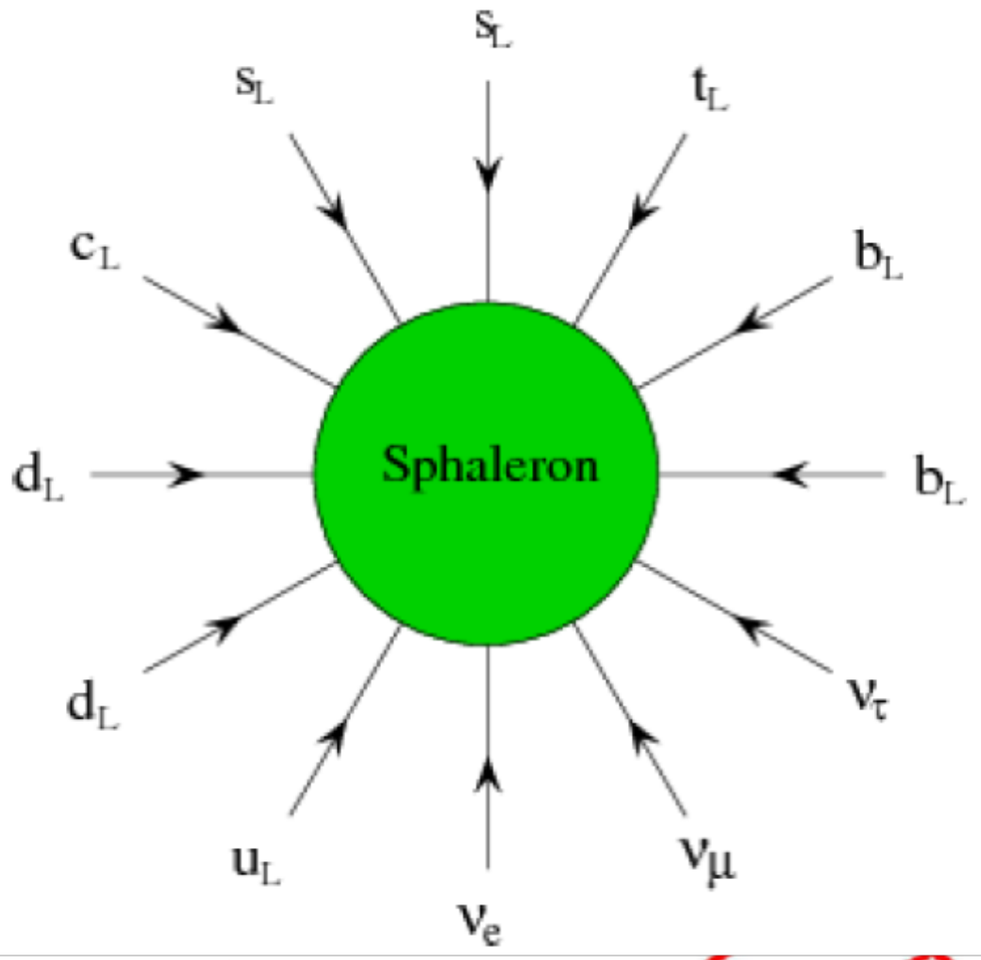

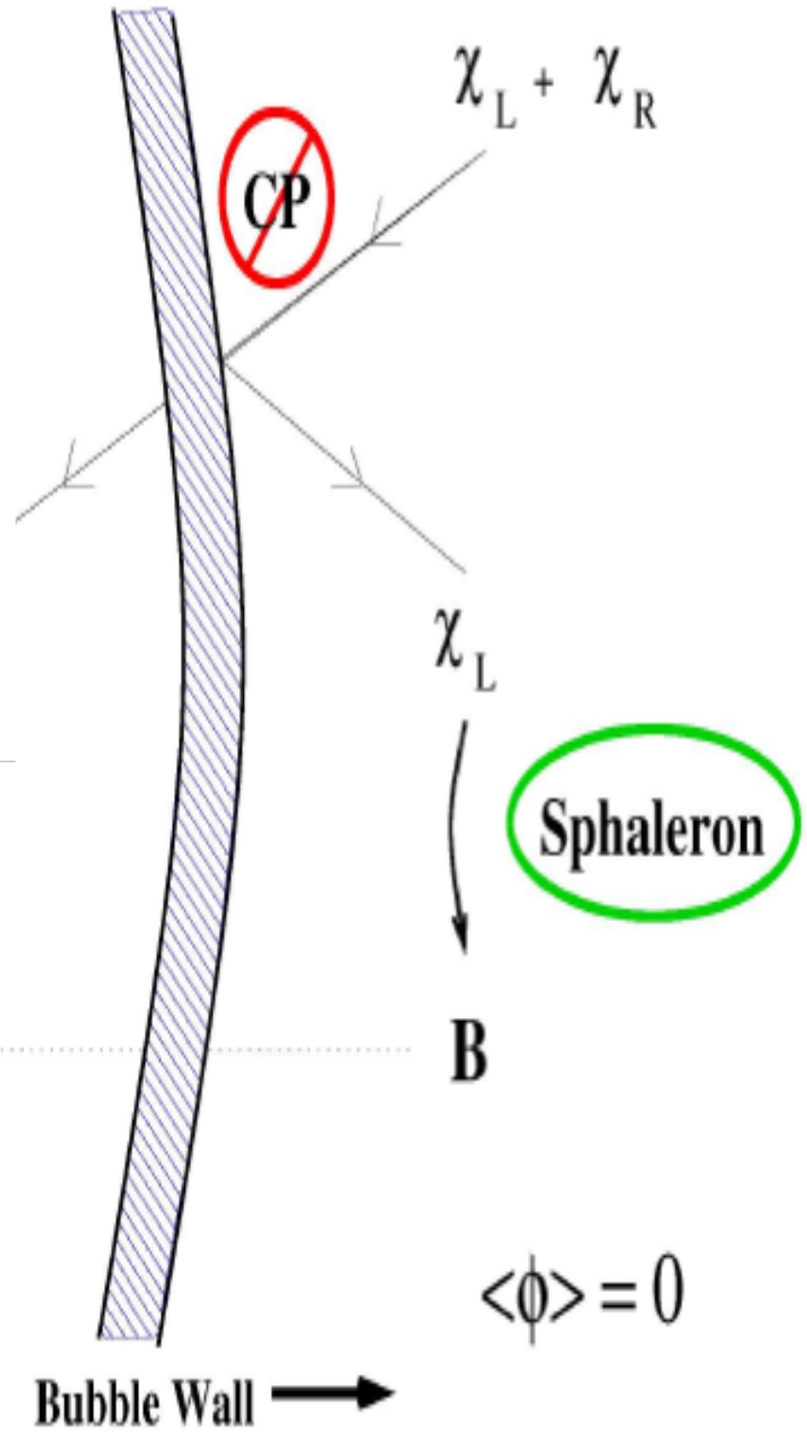

- **B violation from anomaly in B+L current.**
- **CKM matrix, but too weak.**
- **strong first-order phase transition (SFOPT) with expanding Higgs Bubble wall.**

D. E. Morrissey and M. J. Ramsey-Musolf, New J. Phys. 14, 125003 (2012).

Phase transition GW in a nutshell

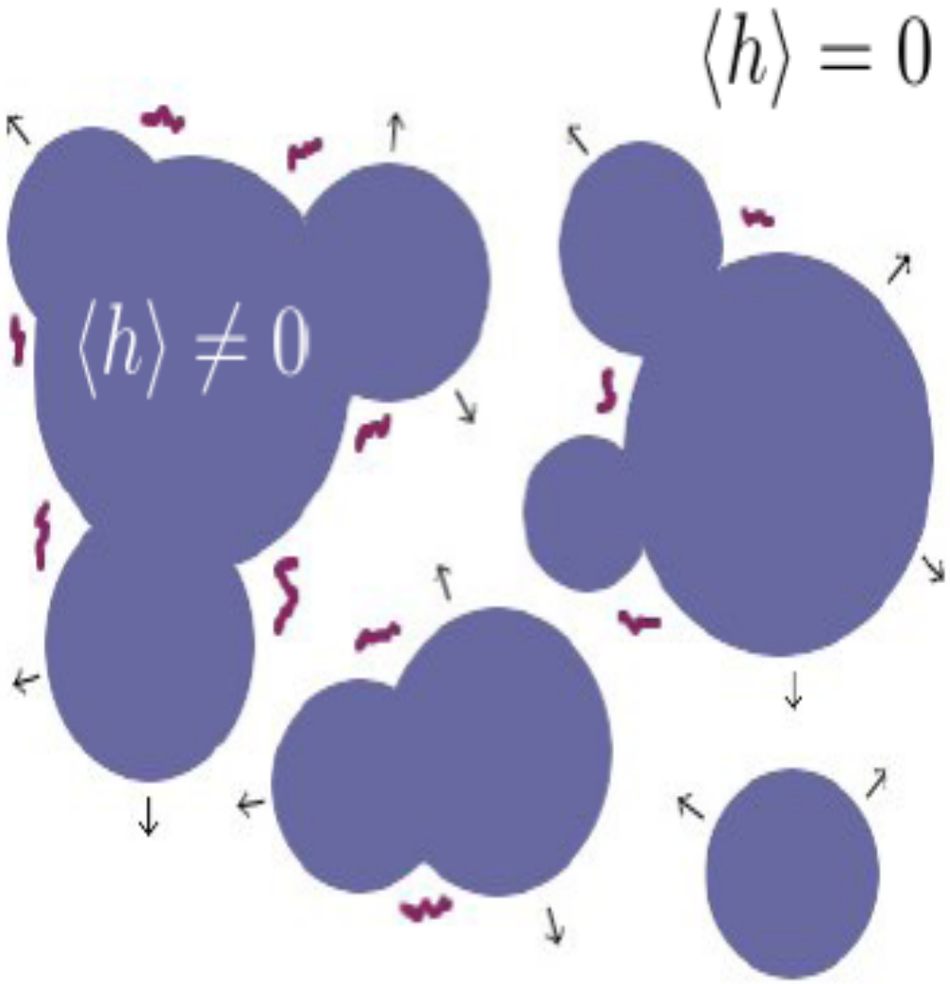

E. Witten, Phys. Rev. D 30, 272 (1984)
C. J. Hogan, Phys. Lett. B 133, 172 (1983);
M. Kamionkowski, A. Kosowsky and M. S. Turner, Phys. Rev. D 49, 2837 (1994))

EW phase transition GW becomes more interesting and realistic after the discovery of Higgs by LHC and GW by LIGO.

Strong First-order phase transition (FOPT) can drive the plasma of the early universe out of thermal equilibrium, and bubbles nucleate during it, which will produce GW.

Mechanisms of GW from phase transition

- **Bubble collision:** **well-known source from 1983**

- **Turbulence in the plasma fluid:** **a fraction of the bubble wall energy converted into turbulence.**

- **Sound wave in the plasma fluid**: **after the collision a fraction of bubble wall energy converted into motion of the fluid (and is only later dissipated). New mechanism of GW：sound wave**

  Mark Hindmarsh, *et al*., PRL 112, 041301 (2014);

Sufficient CP-violation for baryogenesis v.s. electric dipole moment (EDM) measurement

Current EDM data put severe constraints on many baryogenesis models. For example, ACME Collaboration's new result, i.e.

$|d_e| < 1.1\times 10^{-29}$ cm · e at 90% C.L. (Nature vol.562,357,18th Oct. 2018) , has ruled out a large portion of the CP-violating parameter space for many baryogenesis model

$$|d_e| < 8.7 \times 10^{-29}\ \mathrm{cm}\cdot\mathrm{e}$$ **(ACME 2014)**

$$|d_e| \sim< 1 \times 10^{-29}$$ **(ACME 2018)**

Large enough CP-violating source for successful EW baryogenesis

Strong tension in most cases

pretty small CP-violation to avoid strong EDM constraints

How to alleviate this tension for successful baryogenesis?

Question: How to *alleviate* the tension between sufficient CP violation for successful electroweak baryogenesis and strong constraints from current EDM measurements ?

Answer: Assume the CP-violating coupling evolves with the universe. In the early universe, CP violation is large enough for successful baryogenesis. When the universe evolves to today, the CP violation becomes negligible !

Large enough CP-violating source in the early universe for successful EW baryogenesis

alleviate **by assuming the CP-violating source is time dependent**

Dynamical/cosmological evolve

Negligible CP-violating source at current time to avoid strong EDM constraints

- I. Baldes, T. Konstandin and G. Servant, arXiv:1604.04526,
- I. Baldes, T. Konstandin and G. Servant, JHEP 1612, 073 (2016)
- S. Bruggisser, T. Konstandin and G. Servant, JCAP 1711, no. 11, 034 (2017)

First, we study the following case as a representative example:

Phys.Rev. D98 (2018) no.1, 015014 (FPH, Zhuoni Qian, Mengchao Zhang)

$$\mathcal{L}_{\rm SM} - y_t\frac{\eta}{\Lambda}S\bar{Q}_L\tilde{\Phi}t_R + \mathrm{H.c} + \frac{1}{2}\partial_\mu \mathrm{S}\partial^\mu \mathrm{S} + \frac{1}{2}\mu^2\mathrm{S}^2 - \frac{1}{4}\lambda\mathrm{S}^4 - \frac{1}{2}\kappa\mathrm{S}^2(\Phi^\dagger\Phi)$$

$\eta = a + ib$

The singlet and the dim-5 operator can come from many types composite Higgs models
arXiv:0902.1483 , arXiv:1703.10624 ,arXiv:1704.08911,

Firstly, a second-order phase transition happens, the scalar field S acquire a vacuum exception value (VEV) and the dim-5 operator generates a sizable CP-violating coupling for successful baryogenesis.

Secondly, SFOPT occurs when vacuum transits from (0,<S>) to (<Φ>,0).

1. During the SFOPT, detectable GW can be produced.

2. After the SFOPT, the VEV of S vanishes which avoids the strong EDM constraints, and produces abundant collider phenomenology at the LHC and future lepton colliders, such as CEPC, ILC, FCC-ee.

Renormalizable model is working in progress with Eibun Senaha.

J. M. Cline and K. Kainulainen, JCAP **1301**, 012 (2013)

J. R. Espinosa, B. Gripaios, T. Konstandin and F. Riva, JCAP **1201**, 012 (2012)

- I. Baldes, T. Konstandin and G. Servant, arXiv:1604.04526,
- I. Baldes, T. Konstandin and G. Servant, JHEP 1612, 073 (2016)
- S. Bruggisser, T. Konstandin and G. Servant, JCAP 1711, no. 11, 034 (2017)
- S. Bruggisser, B. Von Harling, O. Matsedonskyi and G. Servant, arXiv:1803.08546

Benchmark points, which can give SFOPT and produce phase transition GW

Benchmark set	κ	m_S [GeV]	T_N [GeV]	α	$\tilde{\beta}$
I	2.00	115	106.6	0.035	107
II	2.00	135	113.6	0.04	120

After the first step phase transition, S field obtains a VEV, and then CP-violating top Yukawa coupling is obtained. Thus, during SFOPT, top quark has a spatially varying complex mass

$$m_t(z) = \frac{y_t}{\sqrt{2}} H(z) \left(1 + (1+i)\frac{S(z)}{\Lambda}\right) \equiv |m_t(z)| e^{i\Theta(z)}$$

$$\eta_B = \frac{405\Gamma_{\rm sph}}{4\pi^2 \tilde{v}_b g_* T} \int dz\, \mu_{B_L} f_{\rm sph}\, e^{-45\,\Gamma_{\rm sph}|z|/(4\tilde{v}_b)}$$

Differences between relative velocity and bubble wall velocity for baryogenesis and GW in deflagration case.

We choose reasonably small relative velocity $\tilde{v}_b$~ 0.2, which is favored by the EW baryogenesis to guarantee a sufficient diffusion process in front of the bubble wall, and large enough bubble wall velocity $v_b \sim 0.5$ to produce stronger phase transition GW (Roughly speaking, for deflagration case, a larger bubble wall velocity v_b gives stronger GW)

$$\tilde{v}_b(0.2) < v_b(0.5) < c_s(\sqrt{3}/3)$$

- J. M. No, Phys. Rev. D 84, 124025 (2011)

From the roughly numerical estimation, we see that the observed BAU can be obtained as long as $\Delta\sigma/\Lambda \sim 0.1 - 0.3$, where $\Delta\sigma$ is the change of σ during the phase transition

Particle phenomenology induced by CP-violating top loop

After SM Higgs obtains a VEV v at the end of the phase transition, we have

$$\mathcal{L}_{Stt} = -\left(\frac{m_t}{\Lambda} + \frac{m_t H}{\Lambda v}\right) S\left(a\bar{t}t + ib\bar{t}\gamma_5 t\right)$$

The one-loop effective operators can be induced by covariant derivative expansion method

$$\begin{aligned}\mathcal{L}'_{SVV} &= \frac{a\alpha_S}{12\pi\Lambda} S G^a_{\mu\nu} G^{a\mu\nu} - \frac{b\alpha_S}{8\pi\Lambda} S G^a_{\mu\nu} \tilde{G}^{a\mu\nu} \\ &+ \frac{2a\alpha_{EW}}{9\pi\Lambda} S F_{\mu\nu} F^{\mu\nu} - \frac{b\alpha_{EW}}{3\pi\Lambda} S F_{\mu\nu} \tilde{F}^{\mu\nu}\end{aligned}$$

Mixing for H and S comes from one-loop contribution.

Abundant collider signals

I. Hadron collider:

$$pp \to HS$$

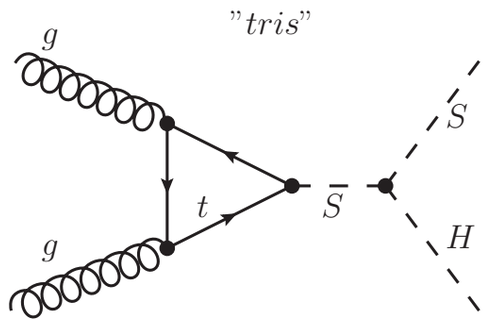

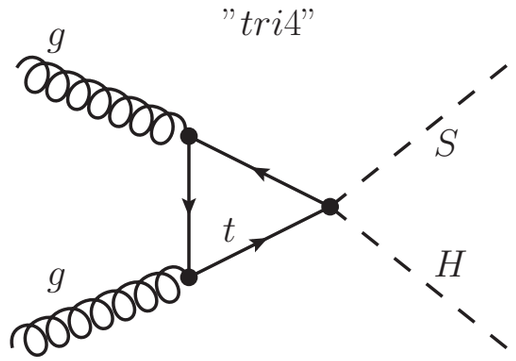

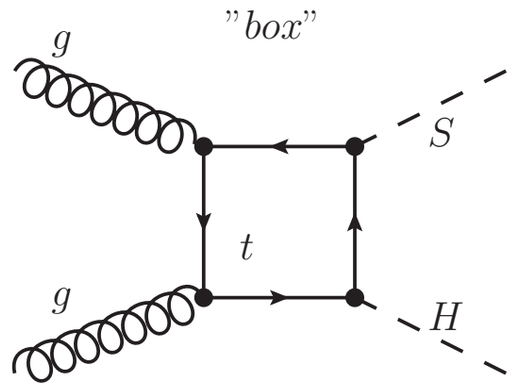

II. Lepton collider (CEPC for example):

1. Direct search: ZS production recoiled muon pair mass distribution:

$$\sigma(e^+e^- \to ZS) = \frac{G_F^2 m_Z^4}{96\pi s}(v_e^2 + a_e^2)|\mathcal{O}_{12}|^2\sqrt{\tilde{\lambda}}\ \frac{\lambda + 12m_Z^2/s}{(1 - m_Z^2/s)^2}$$

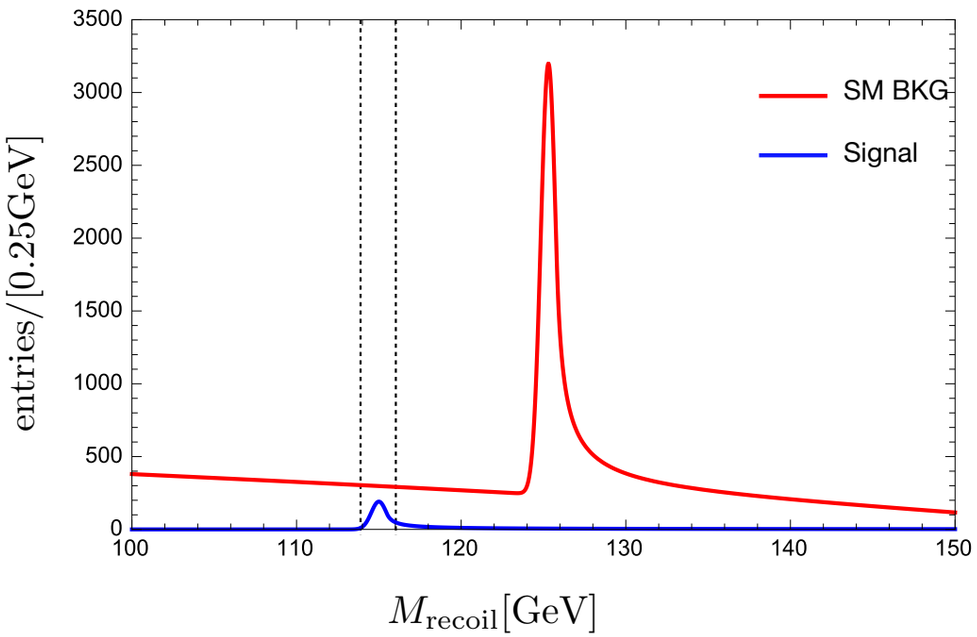

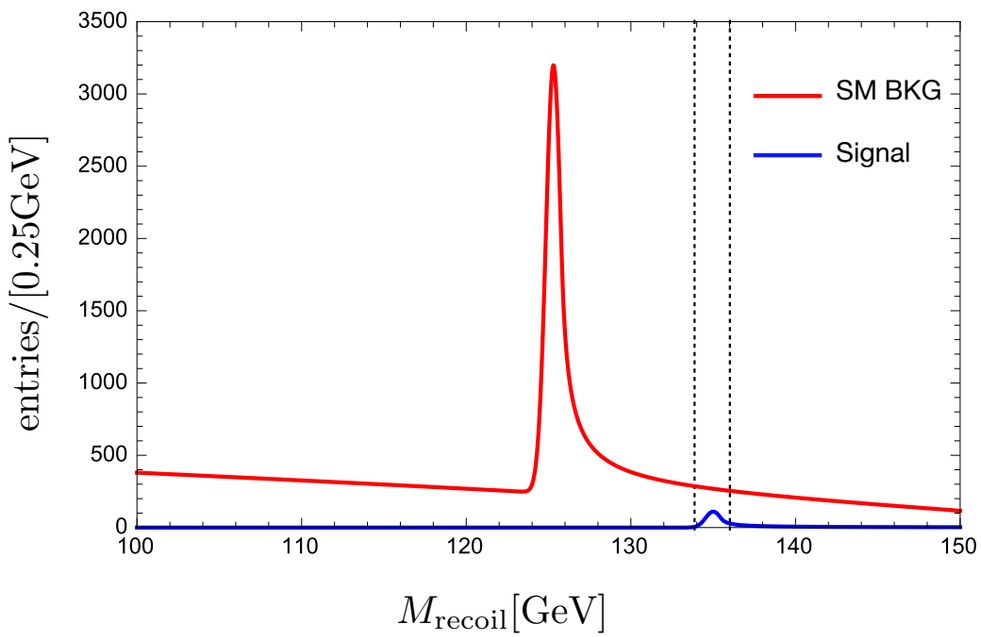

2. Indirect search: ZH cross section deviation from mixing and field strength renormalization:

$$\mathcal{Z} = 1 + \frac{\kappa^2 v^2}{32\pi^2 m_H^2}\left(1 - \frac{4m_S^2}{m_H^2}\frac{1}{\sqrt{\frac{4m_S^2}{m_H^2} - 1}}\arctan\frac{1}{\sqrt{\frac{4m_S^2}{m_H^2} - 1}}\right)$$

$$\text{So } \sigma(e^+e^- \to HZ) \text{ will be rescaled by a factor } |\mathcal{O}_{22}|^2\mathcal{Z}$$

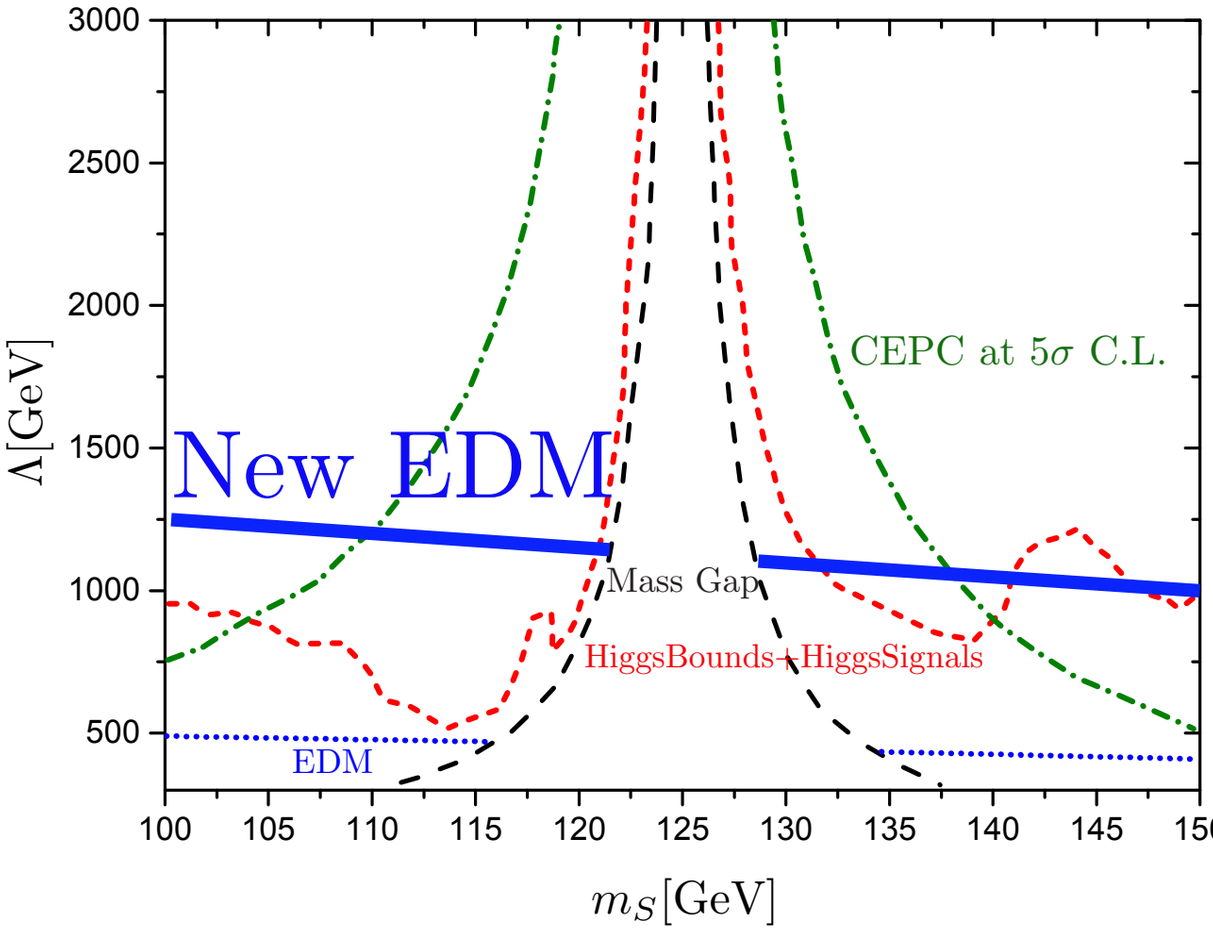

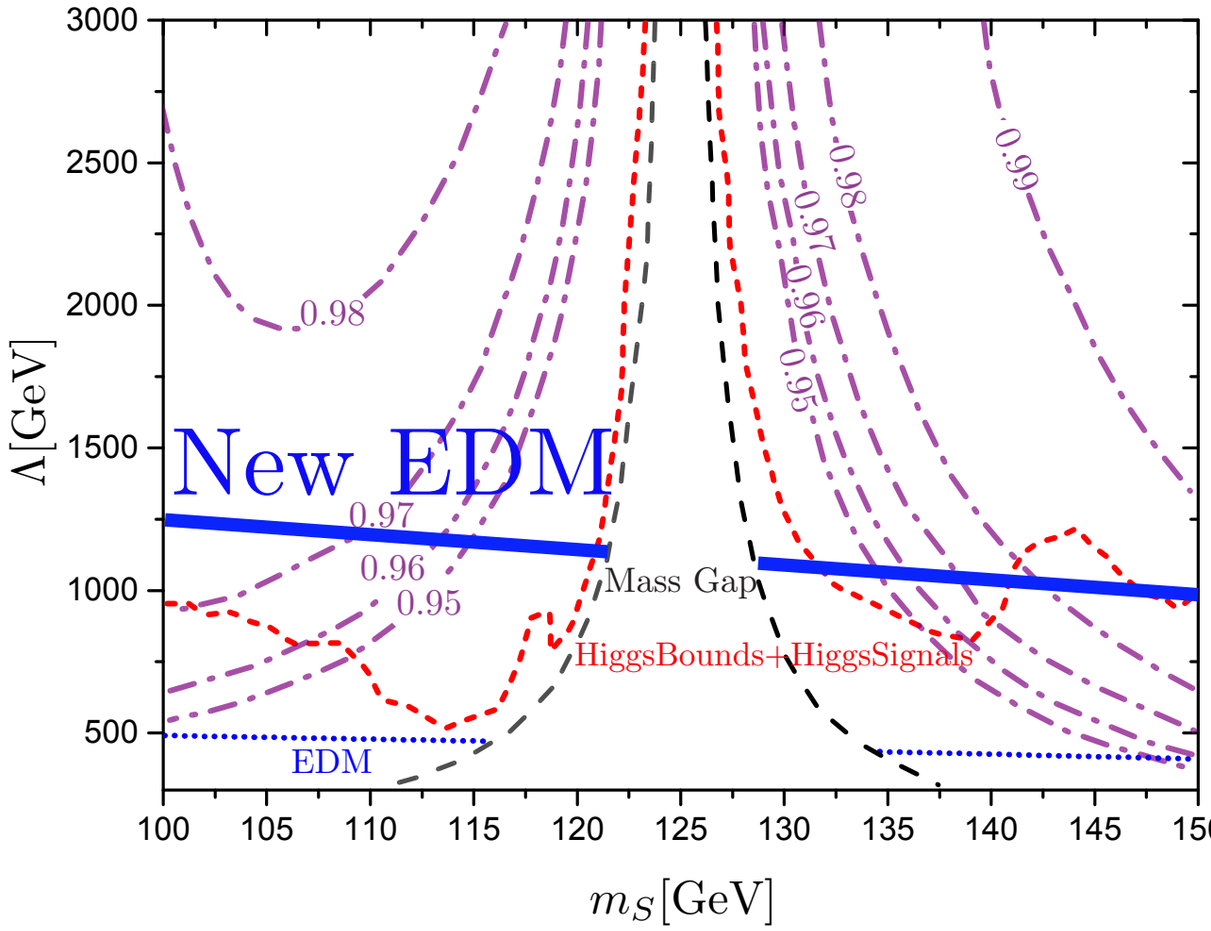

Current exclusion limit and future search sensitivity projected on Λ versus ms plane. The regions below dotted blue lines have been excluded by EDM measurement; regions below dashed red lines have been excluded by collider scalar searches and Higgs data. In the left plot, regions below dash dotted olive lines can be observed from ZS production at 5 ab^{-1} CEPC with a C.L. higher than 5σ. In the right plot, we show the ratio of ZH cross section with purple dash dotted contour lines.

N.B. Limit from EDM is much weaker than Higgs data, due to the fact the contributions to EDM in this scenario come from three-loop contributions

The correlation between the future GW and collider signals

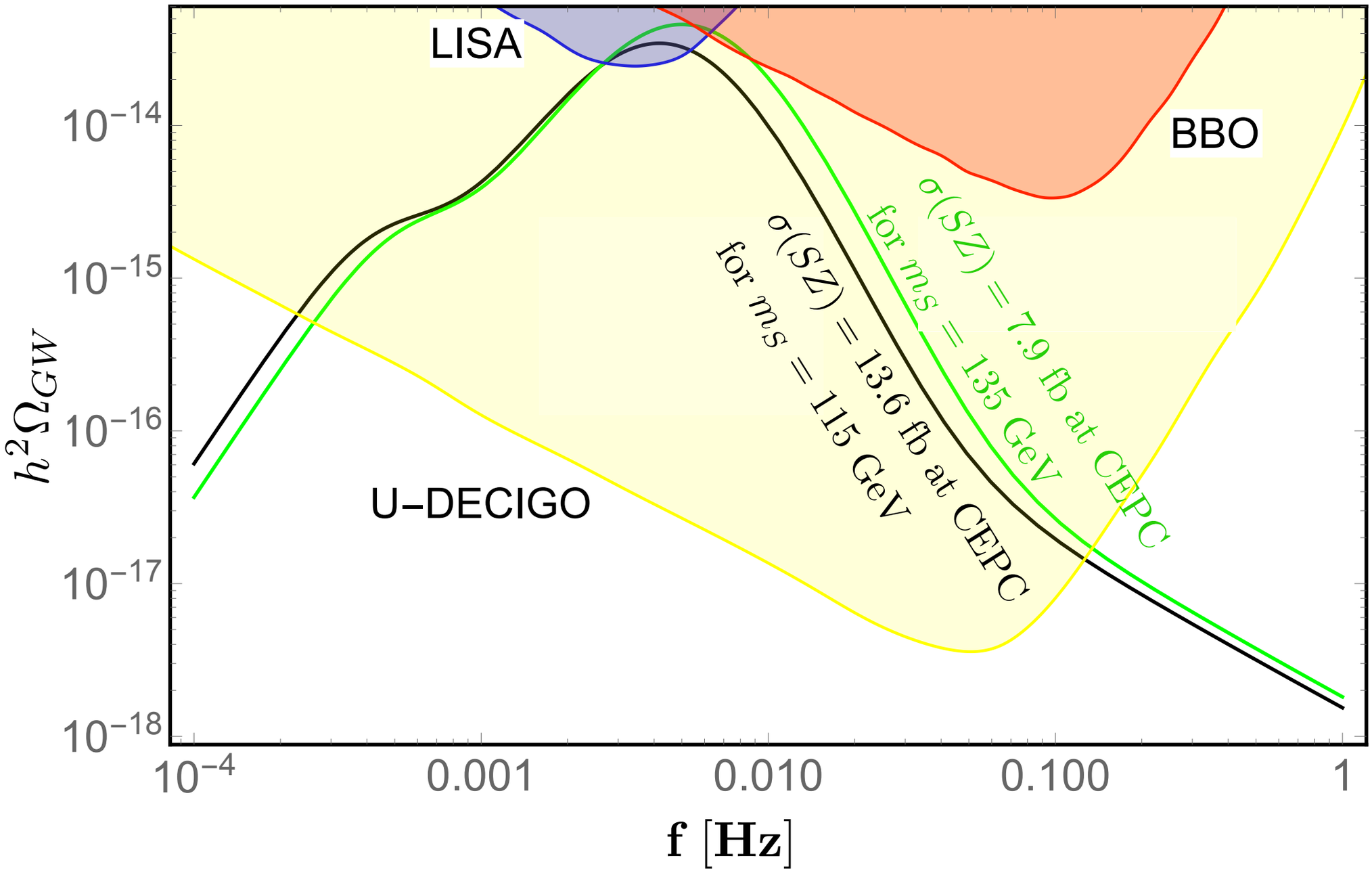

For example taking benchmark set I, the GW spectrum is represented by the black line, which can be detected by LISA and U-DECIGO. The black line also corresponds to $0.9339\sigma_{SM}(HZ)$ of the HZ cross section for $e^+e^- \to HZ$ process and 115 GeV recoil mass with 13.6 fb cross section for the $e^+e^- \to SZ$ process, which has a 5σ discovery potential with 5 ab^{-1} luminosity at CEPC.

More general

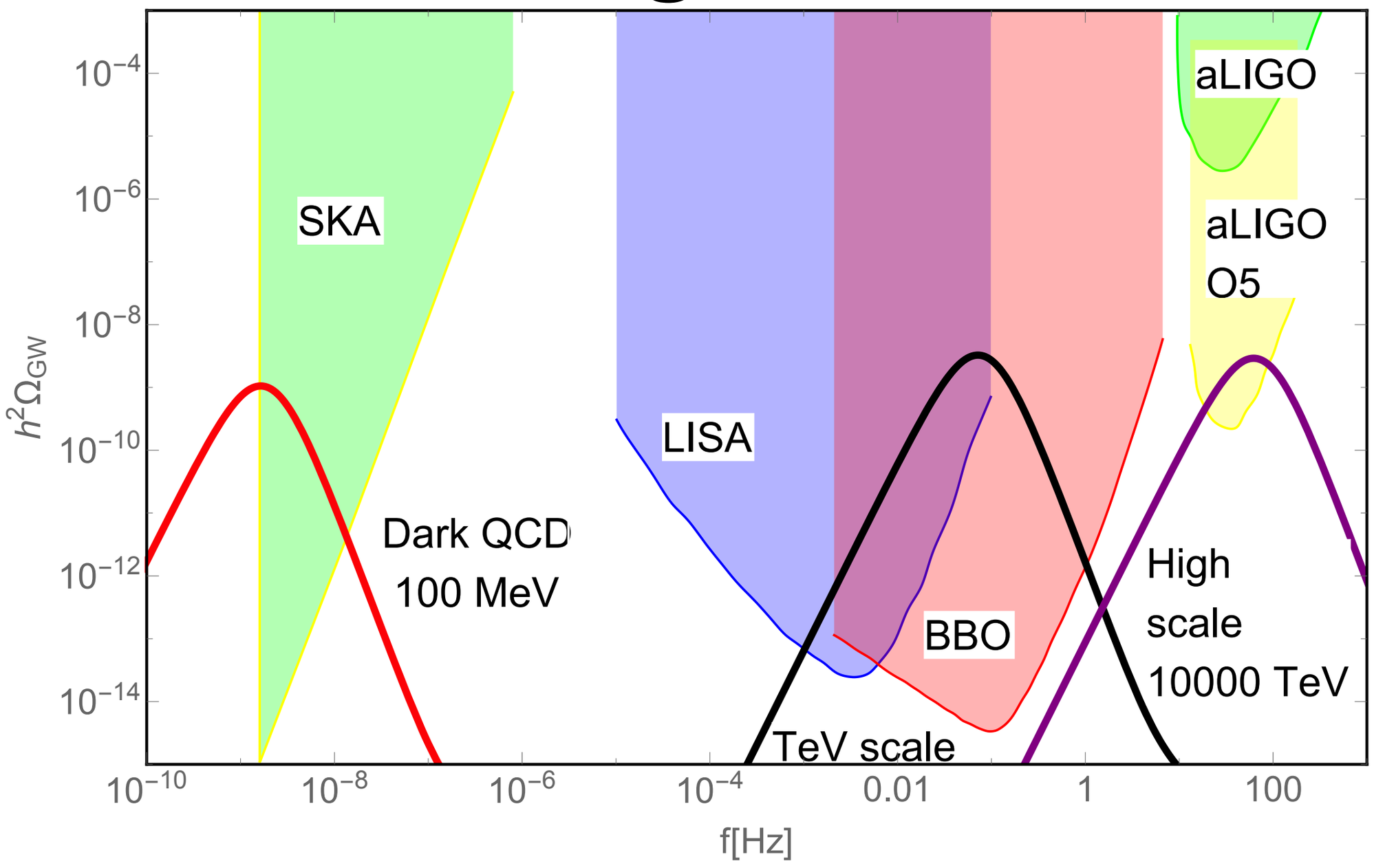

Schematic phase transition GW spectra for SKA-like and LISA-like experiments to detect dark matter and baryogenesis

FPH, Xinmin Zhang, Physics Letters B 788 (2019) 288-294

arXiv:1905.00891,P. S. Bhupal Dev, Francesc Ferrer, Yiyang Zhang, Yongchao Zhang

arXiv:1602.04203,P. S. Bhupal Dev, A.Mazumdar

*Axion cold dark matter

Conclusion

The SKA-like and LISA-like experiments (more and more experiments, SKA, FAST, GBT, LISA, Tianqin/ Taiji) can provide new approaches to explore the nature of dark matter and baryon asymmetry of the universe.

Thanks for your attention!

$m_a \sim m_\gamma$

Comments and collaborations are welcome!